The Journal of Immunology

Self-Antigens Displayed on Liposomal Nanoparticles above a Threshold of Epitope Density Elicit Class-Switched Autoreactive Antibodies Independent of T Cell Help

Zhilin Chen, Wei-Yun Wholey, Alireza Hassani Najafabadi, James J. Moon, Irina Grigorova, Bryce Chackerian and Wei Cheng

J Immunol published online 13 December 2019
http://www.jimmunol.org/content/early/2019/12/12/jimmunol.1801677

The Journal of Immunology is published twice each month by
The American Association of Immunologists, Inc.,
1451 Rockville Pike, Suite 650, Rockville, MD 20852

Print ISSN: 0022-1767 Online ISSN: 1550-6606.

Published December 13, 2019, doi:10.4049/jimmunol.1801677

Self-Antigens Displayed on Liposomal Nanoparticles above a Threshold of Epitope Density Elicit Class-Switched Autoreactive Antibodies Independent of T Cell Help

Zhilin Chen,* Wei-Yun Wholey,* Alireza Hassani Najafabadi,* James J. Moon,*,† Irina Grigorova,‡ Bryce Chackerian,§ and Wei Cheng*,¶

Epitope density has a profound impact on B cell responses to particulate Ags, the molecular mechanisms of which remain to be explored. To dissect the role of epitope density in this process, we have synthesized a series of liposomal particles, similar to the size of viruses, that display a model self-antigen peptide at defined surface densities. Immunization of C57BL/6J mice using these particles elicited both IgM and class-switched IgG1, IgG2b, and IgG3 autoreactive Abs that depended on the epitope density. In C57BL/6 gene knockout mice lacking either functional TCRs or MHC class II molecules on B cells, the liposomal particles also elicited IgM, IgG1, IgG2b, and IgG3 responses that were comparable in magnitudes to wild-type mice, suggesting that this B cell response was independent of cognate T cell help. Notably, the titer of the IgG in wild-type animals could be increased by more than 200-fold upon replacement of liposomes with bacteriophage Qβ virus-like particles that displayed the same self-antigen peptide at comparable epitope densities. This enhancement was lost almost completely in gene knockout mice lacking either TCRs or MHC class II molecules on B cells. In conclusion, epitope density above a threshold on particulate Ags can serve as a stand-alone signal to trigger secretion of autoreactive and class-switched IgG in vivo in the absence of cognate T cell help or any adjuvants. The extraordinary immunogenicity of Qβ viral-like particles relies, in large part, on their ability to effectively recruit T cell help after B cell activation. ***The Journal of Immunology*****, 2020, 204: 000–000.**

Often, foreign particulate Ags such as viral particles can effectively prime the immune system for elicitation of protective Ab responses, with a few exceptions. This B cell response forms the basis for the majority of licensed antiviral vaccines (1). However, how a particulate Ag such as a viral particle activates the immune system to bring about the protective Ab responses, especially at quantitative and mechanistic level, remains largely uncharacterized. A breakthrough in our understanding of this process was put forward by Bachmann et al. (2), who showed that Ag organization had a profound impact on B cell responses to Ags. Remarkably, the envelope glycoprotein displayed on the surface of vesicular stomatitis virus broke the tolerance of B cells in transgenic mice that expressed the same glycoprotein under the control of *H-2K* promoter (2). Along a similar vein, studies led by Schiller and colleagues (3–5) showed that potent and long-lasting autoreactive IgG Abs were elicited in mice upon immunization with self-antigens incorporated or conjugated to papillomavirus-like particles. These discoveries have led to potentially exciting applications in efforts to elicit therapeutic Abs through vaccination approach (6, 7). However, at a fundamental mechanistic level, there remain questions unanswered regarding the extraordinary immunogenicity of these viruses or viral-like particles. Specifically, what are the molecular components or quantitative features in these particles that are required for the potent B cell activation? If collaboration with other immune cells is also required to yield the Ab response, to what extent does the production of these Abs rely on those cells? Answers to these questions will help the design and engineering of vaccines and assist in understanding the spectra of host immune responses to viral pathogens.

Among various features shared by the particles listed above, epitope density appears to be a dominant parameter in the quality of the Ab response. Ensemble estimations based on RNA and proteins present in viral particles yielded ∼500 glycoproteins per vesicular stomatitis viral particle (8), whereas papillomavirus displayed 360 copies of the major capsid protein L1 per particle based on a cryoelectron microscopy study (9). Thus, both viruses display high number of viral-specific epitopes per particle, which is, in fact, a feature shared by most of the human viral pathogens with licensed vaccines (1). Furthermore, Chackerian et al. (3)

*Department of Pharmaceutical Sciences, University of Michigan, Ann Arbor, MI 48109; †Department of Biomedical Engineering, University of Michigan, Ann Arbor, MI 48109; ‡Department of Microbiology and Immunology, University of Michigan, Ann Arbor, MI 48109; §Department of Molecular Genetics and Microbiology, School of Medicine, University of New Mexico, Albuquerque, NM 87131; and ¶Department of Biological Chemistry, University of Michigan Medical School, Ann Arbor, MI 48109

ORCIDs: 0000-0002-1738-0332 (Z.C.); 0000-0002-8215-4374 (A.H.N.); 0000-0002-4963-7403 (I.G.); 0000-0003-0332-1566 (W.C.).

Received for publication December 26, 2018. Accepted for publication November 11, 2019.

This work was supported by the National Institutes of Health (Grant 1R21AI135559-01A1 to W.C.), Mcubed Project 8290, and a Team Science Award from the University of Michigan (to W.C.). Z.C. was partially supported by a Summer Award from the Rackham Graduate School at the University of Michigan.

Address correspondence and reprint requests to Prof. Wei Cheng, University of Michigan, 428 Church Street, Ann Arbor, MI 48109-1065. E-mail address: chengwe@umich.edu

The online version of this article contains supplemental material.

Abbreviations used in this article: BCA, bicinchoninic acid; CSR, class-switch recombination; DLS, dynamic light scattering; DMPC, 1,2-dimyristoyl-sn-glycero-3-phosphocholine; DSPE-PEG (2000) maleimide, 1,2-distearoyl-sn-glycero-3-phosphoethanolamine-*N*-(maleimide [polyethylene glycol]-2000) ammonium salt; $MCII^{-/-}$, MHC class II–deficient; NP-Ficoll, (4-hydroxy-3-nitrophenyl) acetyl–Ficoll; p-liposome, peptide-conjugated liposomal particle; p-$liposome_{1.1\%\text{-m}}$, p-liposome prepared with 1.1% maleimides; p-$liposome_{20\%\text{-m}}$, p-liposome prepared with 20% maleimide lipids; p-$VLP_{Q\beta}$, peptide-conjugated $VLP_{Q\beta}$; SMPH, succinimidyl-6-([β-maleimidopropionamido]hexanoate); $TCR^{-/-}$, TCR-deficient; $VLP_{Q\beta}$, bacteriophage Qβ viral-like particle.

showed that reduction of epitope density on papillomavirus-like particles significantly decreased the IgG autoantibody production, highlighting the critical role of high epitope density in breaking the B cell tolerance. Similarly, a study by Bachmann and colleagues (10) also showed that epitope density on bacteriophage Qβ viral-like particles ($VLP_{Q\beta}$) strongly influenced the resulting IgG Ab response. However, high epitope density alone does not seem to entail the full story. It was showed early on that very-high density of Ags could induce B cell tolerance both in vitro and in vivo (11, 12). A recent study of mouse B cells also suggested that too-high epitope density in the absence of immediate T cell help might trigger B cell death instead of activation (13).

To understand quantitatively and mechanistically B cell responses to particulate Ags and define the role of epitope density in this process, we have taken a "deconstructive" approach: chemically synthesizing particulate Ags similar to the size of viruses and using these particles for immunization in mice. We chose liposomes as carriers for the epitope of interest for two reasons: 1) the nonimmunogenic nature of liposomes by themselves, and 2) the versatility of liposomes in epitope conjugation and engineering (14). In particular, as we have shown recently (15), epitopes of interest can be conjugated onto the surface of these particles in a controlled fashion that yields particles with varied epitope densities, an important tool to unravel the role of epitope density in this process. As we show, these liposomal particles, in the absence of any adjuvants, can elicit IgG autoreactive Abs in mice that depends on epitope density. To the best of our knowledge, this is the first time that a self-antigen, upon conjugation to liposomes above a threshold of epitope density, is shown to induce IgG Ab responses in the absence of T cell help. Furthermore, replacement of liposomes with $VLP_{Q\beta}$ at comparable epitope densities dramatically enhanced the titer of the IgG response. Studies using gene knockout mice revealed that the superior immunogenicity of Qβ viral-like particles originated, in large part, from their extraordinary ability to recruit MHC class II–dependent T cell help after B cell activation. Our study has thus uncovered a fundamental aspect in B cell activation by particulate Ags and offered valuable insights to future vaccine design targeting self-antigens.

Materials and Methods

Synthesis of liposomes and Ag conjugation

Liposomes were prepared using oil-in-water emulsion precursor, followed by membrane extrusion as described (1–3). Three different lipids of designated molar ratios were used in the synthesis of liposomes: 1,2-dimyristoyl-sn-glycero-3-phosphocholine (DMPC), 1,2-distearoyl-sn-glycero-3-phosphoethanolamine-*N*-(maleimide [polyethylene glycol]-2000) ammonium salt (DSPE-PEG [2000] maleimide), and cholesterol (Avanti Lipids). Briefly, lipid mixture (7.5 μM in total) in chloroform were added to a round-bottom flask, blown dry with purified argon, and desiccated by vacuum to form a thin film at the bottom of the flask. One milliliter HEPES buffer (50 mM HEPES and 150 mM NaCl [pH 6.9]) (16) was added to hydrate the lipid film through vortex and short bursts of sonication in a water bath. After hydration, the lipid film resuspension was extruded using polycarbonate membrane with pore sizes of 1000 and 100 nm sequentially for 10 times each. Synthesized liposomes were incubated with a synthetic peptide of the sequence CSSQNSSDKPVAHVVANHQVE (TNF-α peptide, >95% purity; Biomatik) at a chosen molar ratio between the maleimide functional group and the peptide. The sequence of the peptide was derived from mouse TNF-α. The N-terminal cysteine of the peptide was engineered for the purpose of maleimide conjugation. After overnight incubation at 22˚C, the liposome peptide mixture was applied to Sepharose CL-4B gel-filtration column, as we described previously (15), to separate TNF-α–conjugated liposomes from unconjugated free peptides. To prepare peptide-conjugated liposomes of smaller diameters, the lipid film resuspension was extruded using polycarbonate membrane with pore sizes of 1000 and 50 nm sequentially for 10 times each, and the rest of the procedures were the same as described above. To prepare dual-functional liposomes for flow cytometry analysis of mouse splenocytes, 6% DSPE-PEG (2000) maleimide was included in the lipid mixture. The lipid thin film was hydrated using a solution of 0.6 mM Alexa Fluor 594 NHS Ester freshly dissolved in PBS. After extrusion, the liposomes encapsulating Alexa Fluor 594 dye molecules were loaded onto Sepharose CL-4B gel-filtration column to purify liposomes away from excess fluorescent dyes. The eluted liposomal fractions were concentrated by centrifuge through Amicon Ultra-4 Centrifugation unit (100-kDa cutoff) and then mixed with TNF-α peptide for conjugation overnight at 22˚C. The free peptide was removed on the second morning by running liposomes through a Sepharose CL-4B gel-filtration column a second time. The peptide-conjugated liposomes were stored at 4˚C in PBS.

Quantitation of average peptide density on liposomes

The average density of TNF-α peptide covalently conjugated on liposomes was quantitated using the method that we established previously (15). Briefly, we estimate the concentrations of liposome and peptide, respectively, for the liposomes purified through gel-filtration column. The ratio between the two concentrations represents the average number of TNF-α peptide per liposome (15). To estimate the concentration of liposomes, we used the established Stewart assay (17) to determine the phospholipid content in the purified liposomes, based on which the molarity of the liposomes can be further estimated as described (15). Briefly, for each liposomal sample, 20 μl purified liposomes were added to 500 μl of chloroform in a clean glass tube, and then, 500 μl ferrothiocyanate solution containing 0.1 M ferric chloride hexahydrate and 0.4 M ammonium thiocyanate was added. The mixture was vigorously vortexed for 20 s and then centrifuged for 10 min at 1000 × *g* at 22˚C. The lower chloroform layer was then taken for absorption measurement at 470 nm. The phospholipid concentration was calculated based on standard curves constructed from known quantities of DMPC and DSPE-PEG (2000) maleimide, respectively, taking into account the compositions of the two lipids in the liposome samples. To measure the concentration of TNF-α peptide–conjugated on liposomes, we used bicinchoninic acid (BCA) protein assay (18). Briefly, 100 μl of the liposome sample was incubated with 2 ml BCA solution at 60˚C for 30 min before absorption measurement at 562 nm. A total of 8% SDS was also included in this mixture to minimize the interference of lipids to BCA assay as reported (19). The TNF-α peptide concentration was calculated based on the comparison with a standard curve constructed from known quantities of the TNF-α peptide under the same BCA assay conditions.

Stability of epitope density in serum-containing media

Peptide-conjugated liposomes containing 20% of maleimide lipid were chosen for stability studies, as described below. An equal volume of FBS was added to peptide-conjugated liposomes to reach 50% serum condition and incubated at 37˚C. After 1, 3, 5, and 7 d of incubation, respectively, a fraction of liposome-serum mixture was taken and loaded onto Sepharose CL-4B gel-filtration column for purification of liposomes away from serum components. After purification, the liposomes were evaluated using Stewart assay for quantitation of lipid concentration. Incubation with serum may lead to the binding of serum proteins on liposomal surface. Thus, the protein-based BCA assay was no longer reliable in quantitating the amount of peptide conjugated on liposomes. We therefore used an alternative approach based on silver staining of a denaturing polyacrylamide gel to quantitate TNF-α peptides conjugated on liposomes. Liposomes from different time points of serum incubation were normalized based on lipid content and loaded onto a tricine–SDS polyacrylamide gel (20) for electrophoresis. For optimal resolution, we used 16% acrylamide separating gel with 1 cm of 10% spacer gel and 4% stacking gel. The gel was run at 120 V for the initial 20 min, followed by 180 V for the remainder of the time. Silver staining was then carried out for quantitation of peptides on the gel based on the intensity of staining as we reported previously (15).

Conjugation of TNF-α peptide to $VLP_{Q\beta}$

The $VLP_{Q\beta}$ were prepared as described (21). The TNF-α peptide, which contained a single cysteine at its N terminus, was conjugated to the surface of the viral-like particles using the heterobifunctional cross-linker succinimidyl-6-([β-maleimidopropionamido]hexanoate) (SMPH). Briefly, the viral-like particles were first derivatized with SMPH at a 10-fold molar excess of SMPH over Qβ coat protein. The mixture was incubated at 22˚C for 2 h, and the excess cross-linker was removed by centrifugation at 4˚C in an Amicon Ultra-4 centrifugal unit with a 100-kDa cutoff. The TNF-α peptide was then added to the derivatized viral-like particles at a molar ratio of 10:1 over Qβ coat protein. The mixture was incubated at 4˚C overnight, and again, the excess peptide was removed by centrifugation at 4˚C in an Amicon Ultra-4 centrifugal unit with a 100-kDa cutoff.

The quantity of conjugated peptide was assessed using a denaturing polyacrylamide gel based on the intensity from silver staining in comparison with a standard curve obtained from the same gel.

Mice immunizations

All animal procedures were approved by the University of Michigan Animal Care and Use Committee. Female C57BL/6 mice (8 wk; The Jackson Laboratory) were used for immunizations. Prior to inoculation, all injection samples were filtered through a membrane with pore size of 0.45 μm to eliminate potential microbial contamination. One-hundred-microliter samples were injected to each mouse s.c., 50 μl on each flank. The immunization was boosted on days 14 and 28 using the same materials. Mouse blood was collected submentally using Microvette serum collection tube (Sarstedt) 3 d before the first injection and 11 d after each inoculation. The serum was harvested by centrifugation at 10,000 × *g* for 10 min and immediately frozen and stored at −20°C.

Two strains of gene knockout mice were purchased from The Jackson Laboratory: $Tcrb^{tm1Mom}/Tcrd^{tm1Mom}$ (no. 002122) and $Ciita^{tm1Ccum}$ (no. 003239). $Tcrb^{tm1Mom}/Tcrd^{tm1Mom}$ (TCR-deficient [$TCR^{-}/^{-}$]) mice were deficient in both αβ and γδ TCRs (22), whereas $Ciita^{tm1Ccum}$ (MHC class II–deficient [$MCII^{-}/^{-}$]) mice did not have MHC class II molecules on the surface of splenic B cells or dendritic cells (23). Gene knockout mice were housed in germ-free environment, and immunization protocol were carried out as described above for C57BL/6 mice.

ELISA

Blood serum was tested for ELISA to quantitate B cell Ab responses to various immunizations. Ninety-six-well plates (Nunc MaxiSorp; Invitrogen) were coated overnight at 4°C with 5 μg/well of TNF-α peptide in PBS. After blocking with 1% BSA (BSA; Thermo Fisher Scientific) in PBS, mouse sera of different dilution factors (1:100, 1:400, and 1:1600) were added to each well for incubation at 22°C for 2 h. After three washes using PBS with 0.05% Tween 20, secondary anti-mouse IgG HRP Ab (no. 616520; Thermo Fisher Scientific) or anti-mouse IgM HRP Ab (no. 626820; Thermo Fisher Scientific) was added in blocking buffer at 1:5000 dilution and incubated for 1 h at 22°C. Following three washes, 100 μl substrate 3,3′,5,5′-tetramethylbenzidine (Thermo Fisher Scientific) was added to each well and incubated in dark for 10 min. The reaction was stopped by addition of 100 μl 2 M sulfuric acid in each well. The OD of each well at 450 nm was measured using a microplate reader (Synergy HT; BioTek Instruments). All the OD values reported were background subtracted by comparison between two wells that were coated with TNF-α peptide and PBS, respectively. Similarly, for ELISA using TNF-α protein as the bait, 200 ng of recombinant murine TNF-α protein (≥98% purity, no. 315-01A; PeproTech) was coated in each well, and the rest of the procedures were carried out as described above.

To determine the titers of anti–TNF-α Abs, we used serial dilution of serum (from 1:100 dilution to 1:1,638,400 by a dilution factor of 4) for ELISA with either TNF-α peptide or the rTNF-α protein. Cutoff values were calculated using the following equation as reported (24): Cutoff = $\bar{X} + SD \times f$, where $\bar{X}$ and SD are the mean and SD of control well OD reading values, and f is the SD multiplier corresponding to different confidence levels. Specifically in our assays, $f = 2.631$ when the number of control wells was four and confidence level was 95%. The titer value was determined as the highest dilution factor of the serum that still yielded OD450 value higher than the above cutoff value in ELISA.

To determine the subclasses of IgG Abs elicited in mice upon immunization by various agents, we used the following secondary Abs during ELISA: goat anti-mouse IgG1 HRP Ab (no. 1071-05; SouthernBiotech), goat anti-mouse IgG2b HRP Ab (no. 1091-05; SouthernBiotech), goat anti-mouse IgG2c HRP Ab (no. 1078-05; SouthernBiotech), and goat anti-mouse IgG3 HRP Ab (no. 1101-05; SouthernBiotech).

To determine the avidity of anti–TNF-α Abs against recombinant mouse TNF-α proteins, the ELISA was conducted as described above except that after incubation of the diluted sera in the wells for 2 h, the plate was washed once using PBS with 0.05% Tween 20. Eight-M urea was then added to the designated wells for incubation for exactly 5 min (5), after which the wells were washed twice, and the regular ELISA procedure was continued. The avidity index was calculated as the ratio of the mean OD values of urea-treated wells to PBS-treated control wells multiplied by 100 (25).

Flow cytometry analysis of mouse splenocytes

At specific time points following mouse inoculation with various agents, mice were euthanized by CO_2 inhalation, followed by rapid dissection of the spleen. Mouse spleens were minced on ice, and a cellular suspension was separated from tissue using a 40-μm cell strainer. RBCs were removed by rapid exposure of mouse splenocytes to ammonium–chloride–potassium lysis buffer followed by washing with FACS buffer (PBS with 2% FBS and 2 mM EDTA). Single-cell suspensions of mouse splenocytes were first incubated with rat anti-mouse CD16/CD32 (no. 553142; BD Pharmingen) on ice for 15 min, followed by incubation with fluorophore-conjugated Abs and/or TNF-α–conjugated liposomes encapsulating Alexa Fluor 594 for 10 min on ice covered by aluminum foil. The cells were washed twice with 200 μl FACS buffer, resuspended in FACS buffer, and fixed in the presence of 2% PFA at 22°C for 1 h before data acquisition on a Miltenyi Biotec MACSQuant VYB flow cytometer equipped with three spatially separated lasers (405, 488, and 561 nm) and 10 detection channels. A minimum of 100,000 events were collected for all experiments. The fluorophore-conjugated Abs were Pacific Blue rat anti-mouse CD19 (no. 115526; BioLegend) and FITC rat anti-mouse GL7 Ag (no. 144603; BioLegend). The data were analyzed using FlowJo (BD Biosciences).

Statistical analysis

Statistical analysis was carried out using the Statistics toolbox in MATLAB (MathWorks, Natick, MA). Datasets were analyzed using one- or two-way ANOVA, as described in figure legends. Any p values < 0.05 were considered statistically significant. All values were reported as mean ± SE unless otherwise noted.

Results

Liposome-based particulate Ags that carry epitopes of various densities

To obtain a quantitative and mechanistic understanding of B cell responses to particulate Ags such as viruses, we decided to choose liposomes as our platform for Ag design. The unique advantages of using engineered liposomal particles as opposed to a specific virus are 3-fold: 1) the use of liposomes by themselves will not elicit an immune response and therefore provide a baseline for quantification of immunogenicity; 2) it allows us to use defined components to build a particle that mimic certain features of a natural virus particle, and therefore, there is no ambiguity on the constituents of the input Ag; and 3) it allows us to use model Ags, such as the TNF-α peptide used in this study, to systematically investigate the individual contribution of various virus features on B cell responses, including epitope density, the presence or absence of T cell epitope, and TLR ligands, because these different features can be built into a liposomal nanoparticle in a controllable fashion.

In current study, we have selected DMPC as the major lipid for construction of our liposomes, which has a phase transition temperature of 23°C (26) and, therefore, offers ease in extrusion through polycarbonate membranes for formation of unilamellar liposomes. For conjugation of B cell epitopes onto the surface of liposomes, we chose a sequence of 20 aa from mouse TNF-α as our model self-antigen. This peptide corresponds to aa 83–102 of mouse TNF-α. Based on crystal structures of the highly homologous human TNF (27, 28), the C-terminal half of the above peptide is predicted to be solvent exposed and contains critical residues that are directly involved in binding with TNFR (27). Therefore, Abs directed against this peptide are expected to bind the TNF-α protein and potentially block TNF-α and receptor interactions. Indeed, Chackerian et al. (5) were able to elicit potent and long-lasting autoreactive TNF-α Abs in mice using this peptide fused to a truncated form of streptavidin that was conjugated to biotinylated bovine papillomavirus-like particles. Similarly and interestingly, Spohn et al. (29) were able to elicit high titers of Abs in mice that were autoreactive toward soluble, but not membrane-bound, TNF-α protein by conjugation of a similar peptide to viral-like particles of bacteriophage Qβ, suggesting the presence of a mouse B cell epitope in this peptide. The lack of cysteine in the above peptide sequence allowed us to engineer a single cysteine at the N terminus of the peptide for conjugation of this peptide to the surface of liposomes using maleimide chemistry in an orientation

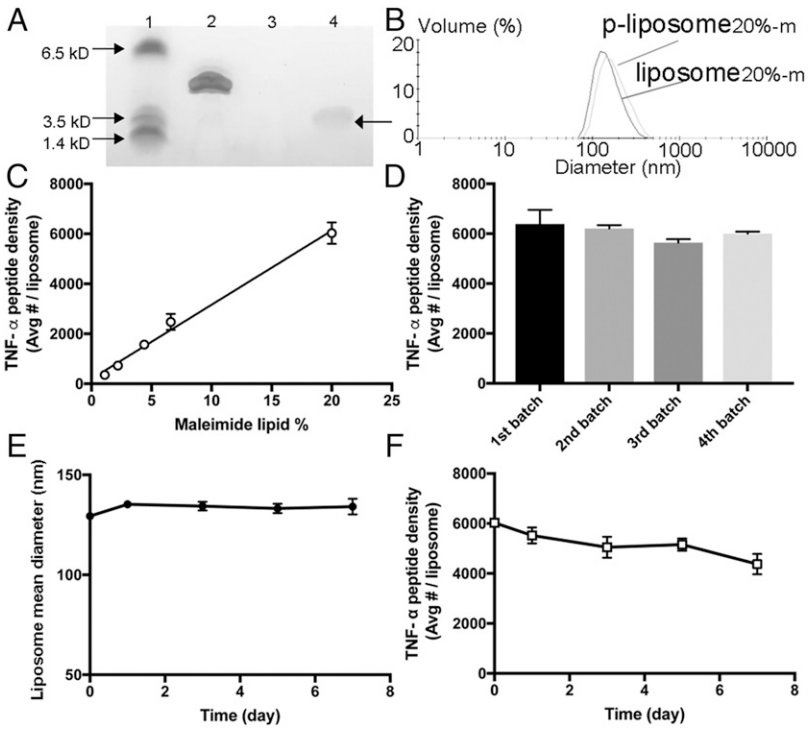

FIGURE 1. Preparation and characterization of p-liposomes of various epitope densities. (**A**) Tricine–SDS-PAGE and silver staining result of samples: lane 1, peptide marker (no. 1610326; Bio-Rad Laboratories); lane 2, 0.12-pmol p-liposome$_{20\%\text{-m}}$; lane 3, 0.12-pmol liposome$_{20\%\text{-m}}$ without peptide conjugation; and lane 4, 1-μg TNF-α peptide. (**B**) DLS size analysis of liposome$_{20\%\text{-m}}$ and p-liposome$_{20\%\text{-m}}$. (**C**) Estimated number of TNF-α peptide per liposome as a function of the maleimide percentage incorporated in liposomes. The error bars represent SDs measured from three independent batches of liposomes prepared with various maleimide percentages listed as follows: 1.1, 2.2, 4.4, 6.6, and 20%. (**D**) Average number of TNF-α peptide molecules per liposome for four batches of p-liposome$_{20\%\text{-m}}$ independently prepared. Error bars represent the SD from two independent estimations of the epitope density. (**E**) Average diameter of p-liposome$_{20\%\text{-m}}$ upon incubation in 50% serum–containing media as a function of incubation time. The error bars represent SDs from three independent repeats of the same experiment. (**F**) Estimated number of TNF-α peptide per liposome for p-liposome$_{20\%\text{-m}}$ upon incubation in 50% serum for various amount of time. Day 0 is before incubation. The error bars represent SDs from three independent repeats of the same experiment.

that exposed its C-terminal residues. For this maleimide chemistry, we have specifically chosen DSPE-PEG (2000) maleimide as the phospholipid for incorporation into liposomes. The presence of polyethylene glycol chain between the lipid head group and the maleimide moiety can increase the residence time of liposomes in the bodily fluid, as demonstrated for many liposomal systems (30–34).

To check the covalent conjugation of the TNF-α peptide onto the liposomes, we ran a 16% denaturing polyacrylamide gel for the purified liposomes and subjected the gel to silver staining. The peptide itself had a molecular mass of 2.2 kDa (indicated by the arrow in lane 4 in Fig. 1A), and the peptide conjugated with DSPE-PEG (2000) maleimide lipid was expected to have a molecular mass of ∼5.1 kDa, as indicated by the band migrating between 3.5 and 6.5 kDa in lane 2 in Fig. 1A. Thus, this was exactly as expected for a 1:1 conjugation of the peptide onto the lipid. We also characterized these liposomal particles using dynamic light scattering (DLS). As shown in Fig. 1B, the DLS data showed a well-defined peak around 153 nm for the peptide-conjugated particles, which compared with 137 nm for bare liposomes, suggesting that the peptide may form a dense layer on liposomal surface under this set of conditions. Consistent with this notion, quantitation of peptide content in the purified liposomes (*Materials and Methods*) revealed 6030 ± 428 (mean ± SD) molecules of TNF-α peptide per liposome on average, which yielded a density of 8.2×10^4 peptides/μm^2 that was more than 2-fold higher than the epitope density on papillomavirus-like particles (3.2×10^4 molecules/μm^2) (1).

To test the effect of epitope density on B cell responses, it is necessary to prepare liposome particles with varied densities of the antigenic peptides. To this end, we systematically changed the molar percentage of the DSPE-PEG (2000) maleimide included during liposome synthesis from 1.1 to 20%. After conjugation of the TNF-α peptide, these liposomes were purified through gel-filtration column, and the epitope density was measured as described (*Materials and Methods*). As shown in Fig. 1C, the epitope density on these liposomes displayed a monotonic increase with increasing percentage of the DSPE-PEG (2000) maleimide lipids. This dependence was well described with a linear relationship (the black line in Fig. 1C), yielding an R^2 value of 0.9922. Specifically, the epitope density decreased to 360 ± 64 for liposomes containing 1.1% maleimide lipids, which was 6.6-fold lower than the epitope density on papillomavirus-like particles. This procedure has a good reproducibility, as shown in Fig. 1D using liposomes containing 20% maleimide lipids as an example. Four independent repeats of the same synthesis and conjugation procedure all yielded an epitope density around 6000 TNF-α peptides per liposome on average.

Finally, because these peptide-conjugated liposomal particles (p-liposomes) were to be used in vivo for mouse immunizations, it is important that the epitope density is stable in biological milieu so that the data can be interpreted using epitope density with confidence. To this end, we incubated p-liposomes in 50% FBS at 37°C for varied time and then purified liposomes away from serum components using a gel-filtration column. The resulting particles were then characterized in terms of size and epitope density. As shown in Fig. 1E for p-liposomes prepared with 20% maleimide lipids (p-liposome$_{20\%\text{-m}}$), the particles remained relatively constant in their size after exposure to serum-containing medium. Also, the density of TNF-α peptide–conjugated on liposomes remained at a similar level over time (Fig. 1F). Thus, we can interpret our results in terms of epitope density with confidence.

TNF-α peptides conjugated on liposomal surface at high density elicit autoreactive IgG Ab in wild-type mice

To examine whether p-liposomes can elicit autoreactive Abs, we first inoculated mice with p-liposome$_{20\%\text{-m}}$, which displayed 6030 ± 430 TNF-α peptides per liposome on average. Each group of mice received three doses of p-liposome$_{20\%\text{-m}}$, each dose containing 4.5 μg TNF-α peptide. No substance other than p-liposome$_{20\%\text{-m}}$ was included in the injections. Ab responses were measured by ELISA using serum collected 11 d after each inoculation. As shown in Fig. 2A, 2B, p-liposome$_{20\%\text{-m}}$ elicited both IgM and IgG responses toward the TNF-α peptides after just one dose. Both responses were significantly higher than either the PBS or bare

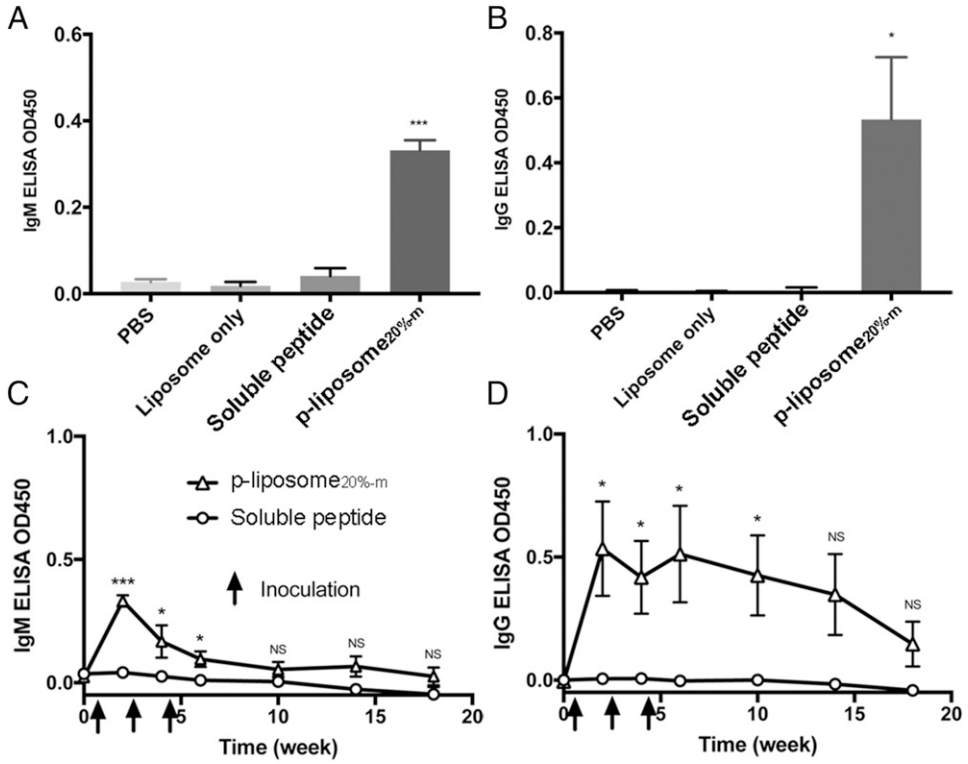

FIGURE 2. Anti–TNF-α peptide Ab response in wild-type C57BL/6 mice. (**A** and **B**) ELISA OD values for IgM (A) and IgG (B) Ab from 1:100 diluted mouse sera after first inoculation using PBS, liposome$_{20\%\text{-m}}$, TNF-α peptide (4.5 μg), and p-liposome$_{20\%\text{-m}}$ containing 4.5 μg peptide. (**C** and **D**) Time courses of ELISA OD values for IgM (C) and IgG (D) from 1:100 diluted mouse sera collected from animals immunized with p-liposome$_{20\%\text{-m}}$ (upper triangle) and the soluble peptide (hollow circle), respectively. The upward arrows denote the time of inoculations. Blood sera were collected at weeks 2, 4, and 6, 11 d after each inoculation, and at weeks 10, 14, and 18 after the first inoculation. Throughout the four panels, each data point in the figure represents the mean of OD450 values obtained from four mice of each group. Error bars represent the SEs. Statistical difference between soluble TNF-α peptide and p-liposome$_{20\%\text{-m}}$ at each time point was determined by Student *t* test. $^{***}p < 0.001$, $^{*}p < 0.05$. NS, not significant ($p > 0.05$).

liposome controls and significantly higher than those elicited by soluble TNF-α peptides at the same dose (4.5 μg). In fact, the levels of IgM and IgG responses from the soluble TNF-α peptides were statistically indistinguishable from those of PBS or bare liposome controls, consistent with the fact that this peptide by itself is a bona fide self-antigen, and no apparent Ab responses were elicited upon immunization. The results shown in Fig. 2A, 2B also suggest that upon conjugation of the peptide to a liposomal nanoparticle, it became immunogenic and could induce class-switched IgG Ab responses, although the liposomal nanoparticles by themselves were not immunogenic.

To further examine the Ab responses elicited by p-liposome$_{20\%\text{-m}}$, we continued to measure both IgM and IgG responses at different time points along the process, up until 18 wk after the first inoculation. As shown in Fig. 2C, the IgM response from p-liposome$_{20\%\text{-m}}$ declined after successive injections, and it continued to decline until the levels of responses became indistinguishable from those induced using soluble peptides by week 10. Similarly, the IgG response from p-liposome$_{20\%\text{-m}}$ also declined after successive injections and became indistinguishable from that of the soluble peptide by week 14 (Fig. 2D). This trend of IgG responses after successive inoculations suggest the lack of apparent Ab affinity maturation or B cell clonal expansion, which was in sharp contrast to the boosting effect typically observed for foreign Ags (35).

Elicitation of autoreactive IgG Ab requires a threshold of epitope density

The above results revealed that a self-antigen, once conjugated onto the surface of a liposomal nanoparticle at high density, could elicit both IgM and IgG Ab responses that were much higher than those from soluble peptide controls at the same Ag dose in the absence of any adjuvants. To further examine the dependence of this immunogenicity on epitope density, we inoculated C57BL/6 mice using p-liposomes conjugated with varied densities of TNF-α peptide. They were p-liposomes prepared with 6.6% maleimides, p-liposomes prepared with 2.2% maleimides, and p-liposomes prepared with 1.1% maleimides (p-liposome$_{1.1\%\text{-m}}$), which displayed on average 2480 ± 322, 730 ± 92, and 360 ± 64 (mean ± SD) TNF-α peptides per liposome, respectively (Fig. 1C). Together with p-liposome$_{20\%\text{-m}}$ and the soluble peptide control, a total of five groups of mice were inoculated. Throughout these experiments, the peptide dose was kept the same regardless of the Ag carriers (4.5 μg TNF-α peptide per injection). Three inoculations were performed for each group, and the Ab responses were measured starting 11 d after the first inoculation. As shown in Fig. 3A, the IgM response from these various liposomes showed a dependence on epitope density and declined by half at p-liposome$_{1.1\%\text{-m}}$. The IgG response from these liposomes also showed a clear dependence on epitope density and declined with decreasing epitope density (Fig. 3B). Interestingly, the IgG response from p-liposome$_{1.1\%\text{-m}}$ was indistinguishable from background, which was in contrast to the IgM response induced by this immunogen. These results revealed that the IgG response toward the TNF-α peptide was more sensitive to the change in epitope density than IgM responses. In particular, low valence liposomal display (360 ± 64 TNF-α peptides) elicited higher IgM response than the soluble peptide but was incapable of eliciting an autoreactive IgG response, clearly showing the dependence of IgG response on epitope density. Qualitatively, a similar phenomenon was also reported previously by Jegerlehner et al. (10) for foreign epitopes conjugated to viral-like particles.

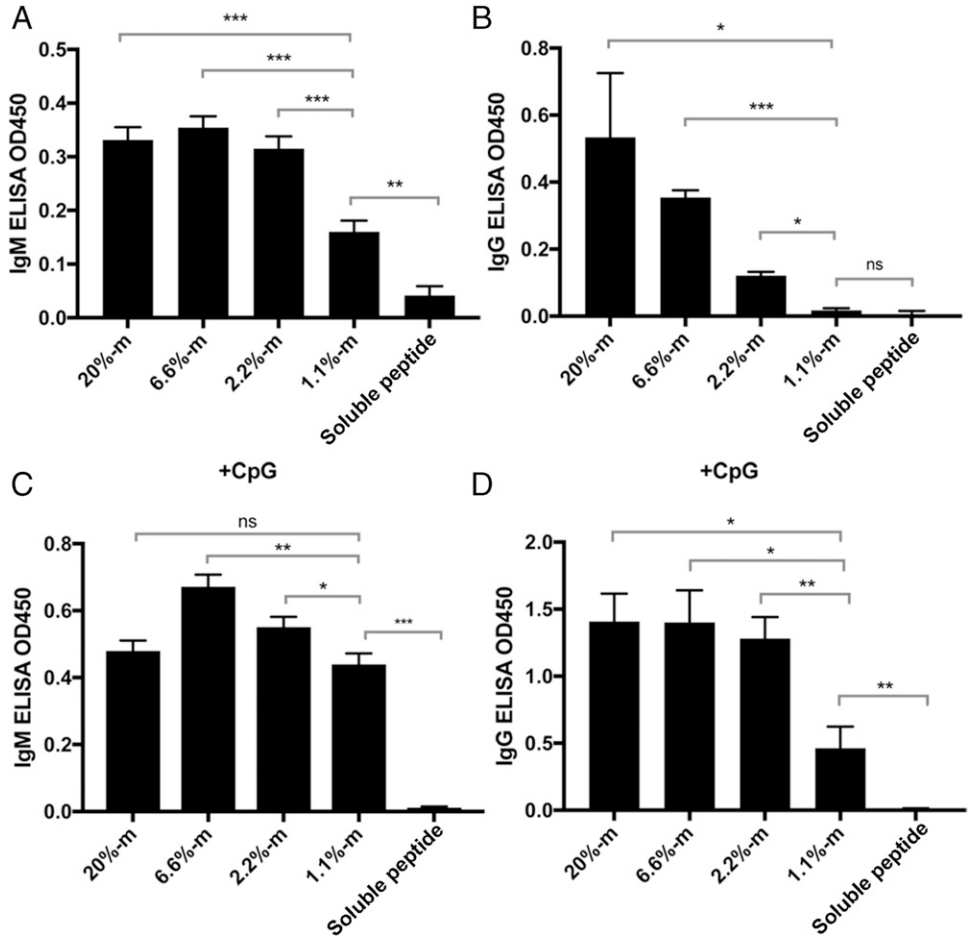

FIGURE 3. Anti–TNF-α peptide Ab response in wild-type C57BL/6 mice measured 11 d after first inoculation with p-liposomes of varied epitope densities. Percentages of maleimide lipid in total lipids are indicated. (**A** and **B**) ELISA OD values for IgM (A) and IgG (B) Ab from 1:100 diluted mouse sera. The dose of TNF-α peptide per injection was the same for all immunizations, 4.5 μg, including the soluble TNF-α peptide. (**C** and **D**) ELISA OD values for IgM (C) and IgG (D) Ab from 1:100 diluted mouse sera. For each inoculation, 20 μg CpG (ODN1826 from InvivoGen) was mixed with various Ags before inoculation. The dose for TNF-α peptide remained 4.5 μg per injection. For all four panels, p-liposome$_{1.1\%\text{-m}}$ was used as a reference to determine statistical difference between data points by Student *t* test. Error bars represent the SEs ($n = 4$). ***$p < 0.001$, **$p < 0.01$, *$p < 0.05$. ns, not significant ($p > 0.05$).

All the immunization experiments reported above were conducted in the absence of other immunostimulatory agents. To examine the effect of TLR activation on these Ab responses, we next performed the above experiments in the presence of CpG, a potent TLR 9 agonist. For each inoculation, 20 μg CpG was mixed with either p-liposomes or the soluble peptide control and then administered into animals. The immunization followed the same schedule as before, and blood was collected at designated time for ELISA. As shown in Fig. 3C, all four p-liposomes induced similar levels of IgM response. The difference of the IgM response between p-liposome$_{1.1\%\text{-m}}$ and other p-liposomes was diminished, suggesting that the presence of CpG weakens the dependence of IgM responses on epitope density. For IgG, three groups of p-liposomes induced similar levels of IgG response (p-liposome$_{20\%\text{-m}}$, p-liposomes prepared with 6.6% maleimides, and p-liposomes prepared with 2.2% maleimides) (Fig. 3D). The IgG response elicited by p-liposome$_{1.1\%\text{-m}}$ remained the lowest among the four groups of liposomes, but in the presence of CpG, its IgG response was clearly detectable above the background and the soluble peptide control. This was in contrast to Fig. 3B, in which p-liposome$_{1.1\%\text{-m}}$ was incapable of eliciting an IgG response above background. These results thus suggest that the presence of CpG likely modulates the sensitivity of B cells to epitope density. Specifically, the presence of CpG may sensitize B cells toward a lower threshold of epitope density that is required to elicit an IgG response. We continued to monitor these animals at later time points. As shown in Supplemental Fig. 1, IgG response did not show any boosting effect upon successive immunizations, which was true for all these liposomal preparations in the absence or presence of CpG, consistent with the patterns we observed in Fig. 2C, 2D.

TNF-α peptides conjugated on Qβ viral-like particles elicit potent autoreactive IgG Ab in wild-type mice

Even in the presence of CpG, it did not escape our attention that the titers of IgG response from these liposomes were only on the order of 1×10^3, which was much lower than the IgG titer reported for the same peptide but noncovalently conjugated to papillomavirus-like particles (5). To examine the mechanisms behind this apparent difference, we conjugated the TNF-α peptide to VLP$_{Q\beta}$ using the heterobifunctional cross-linker SMPH. Bacteriophage Qβ has been used as an Ag presentation platform for elicitation of Abs both in mice and in human clinical trials (21, 36, 37). The single available thiol group present in our synthetic TNF-α peptide allowed us to conjugate this peptide to the surface of SMPH-derivatized VLP$_{Q\beta}$. The excess free peptide was removed by filtration of the reaction mixture through Amicon filtration units. As shown in Fig. 4A, using a silver-stained gel to monitor this conjugation reaction, the SMPH-derivatized VLP$_{Q\beta}$ showed a major band around 15 kDa before

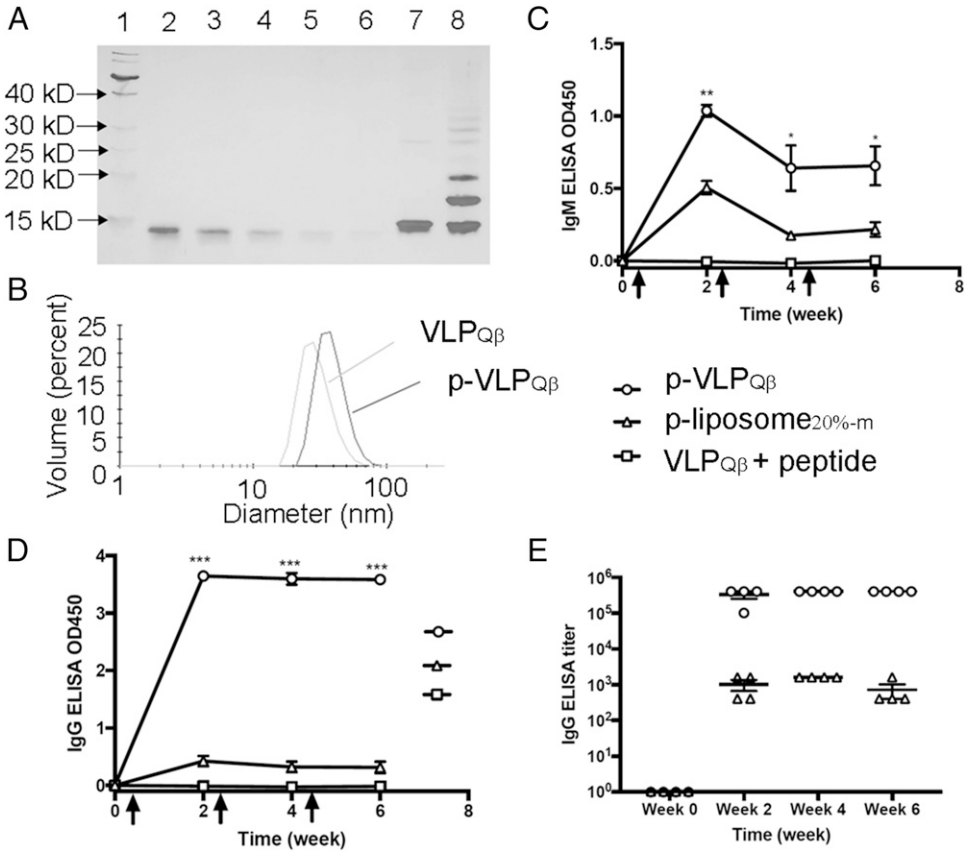

FIGURE 4. Characterization of Qβ particles conjugated with TNF-α peptides and the Ab responses in wild-type C57BL/6 mice immunized with Qβ particles conjugated with TNF-α peptides. (**A**) Tricine–SDS-PAGE and silver staining result of samples listed as follows: lane 1, protein marker (catalog 26614; Thermo Fisher Scientific); lane 2–6, hen egg lysozyme of various quantities (800, 400, 200, 100, and 50 ng, respectively); lane 7, $VLP_{Q\beta}$ (2 μg Qβ); and lane 8, p-$VLP_{Q\beta}$ (4 μg Qβ). (**B**) DLS size analysis of $VLP_{Q\beta}$ and p-$VLP_{Q\beta}$. (**C** and **D**) Time courses of ELISA OD values for IgM (C) and IgG (D) Ab from 1:100 diluted mouse sera upon three successive inoculations using Ags as indicated in the figure. For p-$VLP_{Q\beta}$, the dose of TNF-α peptide was 0.5 μg per injection; for p-$liposome_{20\%\text{-m}}$, the dose of TNF-α peptide was 4.5 μg per injection. The upward arrows denote the time of inoculations. Student *t* test was done to compare p-$VLP_{Q\beta}$ with p-$liposome_{20\%\text{-m}}$. Error bars represent the SEs ($n = 4$). (**E**) IgG titer as a function of time after the first inoculation of the respective Ags as indicated. Each data point represents the IgG titer result from each individual mouse in an immunization group. Lines represent the mean of titers. $^{***}p < 0.001$, $^{**}p < 0.01$, $^{*}p < 0.05$.

conjugation with TNF-α peptide (lane 7), which corresponded to the molecular mass of Qβ coat protein. Upon cross-linking with TNF-α peptide, a series of bands were seen on the gel (lane 8), which matched with the expected molecular masses for the coat protein conjugated with one TNF-α peptide, two TNF-α peptides, and so on. Based on silver staining intensity, we estimated that, on average, there were 260 TNF-α peptides per $VLP_{Q\beta}$. We also characterized these $VLP_{Q\beta}$ using DLS. As shown in Fig. 4B, the DLS data showed a well-defined peak around 42 nm for the peptide-conjugated $VLP_{Q\beta}$ (p-$VLP_{Q\beta}$), which compared with 36 nm for the unconjugated $VLP_{Q\beta}$, suggesting that the peptide formed a dense layer on $VLP_{Q\beta}$ surface that was consistent with our estimation for the average number of peptides per $VLP_{Q\beta}$. These measurements yielded an epitope density of 4.7×10^4 peptides/μm^2 on these p-$VLP_{Q\beta}$, which was comparable to the epitope density on papillomavirus-like particles (3.2×10^4 molecules/μm^2) (1).

We then used the p-$VLP_{Q\beta}$ to immunize C57BL/6 mice. In these experiments, we followed the same immunization schedules as we did for p-liposomes. Also, to compare the immune responses elicited by p-$VLP_{Q\beta}$ to those previously published in literature using papillomavirus-like particles, we used p-$VLP_{Q\beta}$ containing 0.5 μg TNF-α peptides for each inoculation, which was the peptide dose published previously using papillomavirus-like particles. As shown in Fig. 4C, the p-$VLP_{Q\beta}$ elicited 2-fold higher IgM responses than p-$liposome_{20\%\text{-m}}$ containing 4.5 μg TNF-α peptides. Notably, the p-$VLP_{Q\beta}$ elicited IgG responses that saturated the OD reading at 450 nm under the same serum dilution (1:100; Fig. 4D). Control experiments using a simple admixture of $VLP_{Q\beta}$ and the soluble TNF-α peptide at the same particle and peptide doses did not elicit any IgM or IgG response above the background (hollow squares), clearly indicating that it was the conjugation of the TNF-α peptide onto the $VLP_{Q\beta}$ that mattered.

The saturation in OD450 required further dilution of the sera to obtain meaningful titer values for the IgG Ab responses. By performing a serial dilution of the collected sera and repeating the ELISA measurements (*Materials and Methods*), we determined that the IgG response elicited by p-$VLP_{Q\beta}$ had a titer between 1×10^5 and 1×10^6 (Fig. 4E, circles) 11 d after the first inoculation, and these titers were stable after the second and third inoculations. These titer values compared favorably with the titer values previously reported for the same peptide but conjugated to papillomavirus-like particles at the same peptide dose (5). In contrast, the IgG titer elicited by p-$liposome_{20\%\text{-m}}$ was 1×10^3 (Fig. 4E, triangles) 11 d after the first inoculation, and the titer remained at 1×10^3 after the second and third inoculations. No boosting effect was observed for p-liposomes despite the fact that these Ab levels were more than 100-fold lower than those elicited by p-$VLP_{Q\beta}$. These data clearly indicated that p-$VLP_{Q\beta}$ were much more potent than liposomal nanoparticles in eliciting IgG responses.

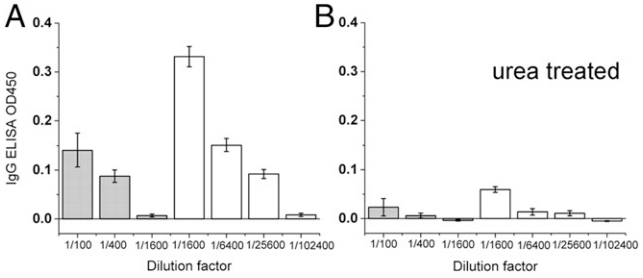

FIGURE 5. Anti–TNF-α protein Ab response in wild-type C57BL/6 mice measured 11 d after first inoculation with either p-liposome$_{20\%\text{-m}}$ or p-VLP$_{Q\beta}$. Sera from mice immunized with p-liposome$_{20\%\text{-m}}$ (4.5 μg TNF-α peptide, gray columns) and p-VLP$_{Q\beta}$ (0.5 μg TNF-α peptide, white columns) were serial diluted as indicated. Each column in the figure represents the mean of OD450 values obtained from four mice of each group ($n = 4$). Error bars represent the SEs. After 2 h of incubation in ELISA plates, the Ag–Ab complexes were treated with either PBS for 5 min (**A**) or 8-M urea for 5 min (**B**), followed by washes and regular ELISA procedures to estimate Ab avidity.

Previous studies by Chackerian et al. (5) showed that the TNF-α peptide–conjugated to papillomavirus-like particles could elicit Abs that were capable of binding to the rTNF-α protein. To test whether our construction of the p-VLP$_{Q\beta}$ could elicit the same effect, we thus conducted ELISA using a rTNF-α protein coated on the ELISA plate. As shown in Fig. 5A, we could clearly detect a positive ELISA signal above background for the sera from p-VLP$_{Q\beta}$–immunized animals at a dilution of 1:25,600. In contrast, a dilution of 1:400 for the serum was required to observe similar OD values for p-liposome$_{20\%\text{-m}}$–immunized animals. Thus, for both p-liposome and p-VLP$_{Q\beta}$, the IgG Abs were able to bind the TNF-α protein, although at different efficiencies. To determine the avidity of the IgG Ab response against the mouse TNF-α protein, we used 8-M urea to treat the Ag–Ab complexes for 5 min after 2 h of incubation, followed by washes and regular ELISA procedures. As shown in Fig. 5B, both IgG responses measured on day 11 after first injection fell significantly after this treatment. Specifically, for sera from p-liposome$_{20\%\text{-m}}$–immunized mice, even at 1:100 dilution, no significant IgG response could be detected above background; for sera from p-VLP$_{Q\beta}$–immunized mice, IgG response could be detected at 1:1600 dilution, but decreased to background levels upon further dilution. These results thus suggest that, on day 11 after first immunization, both IgG responses were still of low avidity, with an avidity index $<30\%$, although both could bind to the recombinant mouse TNF-α proteins.

Why were p-VLP$_{Q\beta}$ much more potent than the aforementioned liposomal nanoparticles in eliciting IgG responses? Among other possibilities, one difference was the size of the particles. The liposomal particles that we so far prepared had diameters around 150 nm, whereas the p-VLP$_{Q\beta}$ were ~3-fold smaller. To examine the effect of particle size on liposomal immunogenicity, we prepared liposomal particles that were ~75 nm in diameter. Again, using 20% maleimide lipids, we conjugated TNF-α peptides to these liposomes at a density of 9.4×10^4 peptides/μm^2 (1720 molecules per liposome on average), similar to our previous p-liposome$_{20\%\text{-m}}$ with peptide density of 8.2×10^4 peptides/μm^2 (6030 ± 428 molecules per liposome). Following the same immunization protocol and using the same peptide dose, we immunized C57BL/6 mice. As shown in Fig. 6, these smaller particles elicited IgM and IgG responses that were very much comparable to those of larger liposomes. Therefore, the size of these particles did not, apparently, explain the huge difference in the immunogenicity between p-VLP$_{Q\beta}$ and p-liposomes.

Ab responses in gene knockout mice lacking cognate T cell help

In general, B cells must receive T help to efficiently proliferate, class switch, and differentiate into long-lived plasma cells. T cells that recognize self-antigens are usually eliminated or tolerized during their maturation (38). Because the TNF-α peptide is a bona fide self-antigen and is the only protein Ag in the liposome-based vaccines, cognate T help may not be available to sustain B cell proliferation. Search of the immune epitope database (www.iedb.org) (39) did not yield any known T cell epitope for this peptide. The lack of boosting effect upon successive inoculations, despite the low-titer values we observed upon a series of p-liposome immunizations (Fig. 2, Supplemental Fig. 1), suggests the lack of T cell help in these IgG responses. In contrast, both the bacteriophage Qβ coat protein and major capsid protein L1 in papillomavirus-like particles are foreign to mice; the inclusion of these proteins in the Ag presentation platforms may have thus served this role of foreign Ags for efficient recruitment of T cell help to sustain B cell activation for more potent IgG response.

To test this hypothesis, we used two different strains of gene knockout mice that were both in the C57BL/6 background (*Materials and Methods*). The first line was deficient in both αβ and γδ TCRs (22) (denoted as TCR^{-}/$^{-}$), whereas the second line did not express MHC class II molecules on the surface of splenic B cells or dendritic cells (23) (denoted as MCII^{-}/$^{-}$), and thus, both lines were deficient in T-dependent B cell activation. We first inoculated these two lines of gene knockout mice using p-liposome$_{20\%\text{-m}}$, following the same immunization schedule and doses as we used for wild-type C57BL/6 mice. As shown in Fig. 7A, these two lines of gene knockout mice produced IgM responses that were identical (within error) to the wild-type C57BL/6 mice. Remarkably, these two lines of gene knockout mice also produced class-switched IgG responses that were similar in magnitudes to the wild-type C57BL/6 mice (Fig. 7B). One-way ANOVA test conducted for these data yielded p values >0.05 for all three groups at weeks 2, 4, 6, 10, 14, and 18, demonstrating that neither IgM nor IgG responses elicited in these animals were statistically different. Furthermore, no boosting effect of IgG response was observed in either of the gene knockout animals, consistent with the result seen in wild-type mice (Fig. 2). These data thus confirmed that the IgG response elicited by p-liposomes in wild-type mice was a result of T-independent B cell activation. These data also showed that class-switched IgG Ab responses against a self-antigen could be elicited by these p-liposomes in the absence of cognate T cell help.

We then used p-VLP$_{Q\beta}$ to immunize the two lines of gene knockout mice, following the schedules and doses that we used for p-liposomes and collected sera at designated time points to measure Ab responses using ELISA. As shown in Fig. 7C, the IgM response from these animals was on the same order of magnitudes in comparison with p-liposome$_{20\%\text{-m}}$. Remarkably, the IgG response from these animals had dropped substantially to a level that could be compared with that elicited by p-liposome$_{20\%\text{-m}}$ (Fig. 7D). By week 6 after the third inoculation, the differences in IgG responses had become insignificant between wild-type mice immunized with p-liposome$_{20\%\text{-m}}$ and gene knockout mice immunized with p-VLP$_{Q\beta}$. This result thus demonstrates that the extraordinary immunogenicity of p-VLP$_{Q\beta}$ is determined, in large part, by the ability of these particles to recruit T cell help after B cell activation.

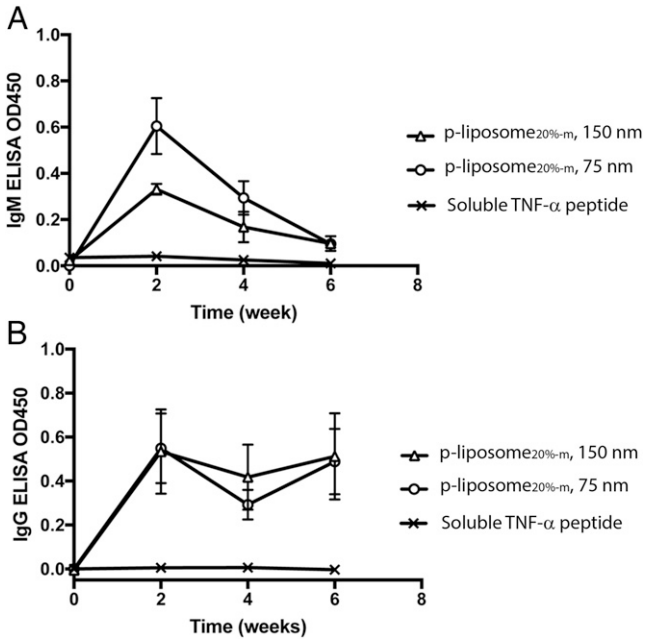

FIGURE 6. Anti–TNF-α peptide Ab response in wild-type C57BL/6 mice as a function of liposomal particle size. Time courses of ELISA OD values for IgM (**A**) and IgG (**B**) from 1:100 diluted mouse sera collected at weeks 2, 4, and 6, 11 d after each inoculation. Each data point in the figures represents the mean of OD450 values obtained from four mice of each group ($n = 4$). Error bars represent the SEs. Data from soluble TNF-α peptide (4.5 μg) were also plotted for comparison (cross).

IgG subclasses of Abs induced upon immunization

To obtain more mechanistic information about the Ab class switching, we determined the subclasses of the IgG Abs induced in mice upon immunization under various conditions. These results are shown in Fig. 8. There are two major observations from these results. First, the TNF-α peptide–conjugated to the surface of liposomes (p-liposome$_{20\%\text{-m}}$) elicited IgG1 Abs in wild-type C57BL/6 (condition 4) together with IgG2b and IgG3. This result was also confirmed in the TCR$^{-/-}$ (condition 5) and MCII$^{-/-}$ (condition 6) gene knockout mice, suggesting that this elicitation of IgG1 can occur in the absence of T cells. Previously, it was shown that T-independent type II Ags such as (4-hydroxy-3-nitrophenyl) acetyl–Ficoll (NP-Ficoll) could induce IgM Abs together with lower amounts of IgG3 and IgG2b, but not IgG1 in C57BL/6 mice (40). Our results in this study thus suggest that the peptide-conjugated liposomal Ags use mechanisms that are distinct from those used by T-independent type II Ags in the induction of class-switched Abs. Second, the peptide-conjugated liposomal Ags did not elicit IgG2c (Fig. 8C). In contrast, the elicitation of IgG2c seems to be well correlated with the presence of nucleic acids in the immunization agents. The TNF-α peptide conjugated to Qβ was administered to wild-type C57BL/6 (condition 8), TCR$^{-/-}$ (condition 9), and MCII$^{-/-}$ (condition 10) mice, respectively. In all cases, IgG2c was strongly elicited (Fig. 8C). Interestingly, when we added CpG DNA oligos to p-liposome$_{20\%\text{-m}}$ in the form of an admixture (condition 11), this agent also induced IgG2c, in sharp contrast to p-liposome$_{20\%\text{-m}}$ alone (condition 4). Throughout, neither liposome only (condition 2) nor the soluble TNF-α peptides (condition 3) elicited any statistically significant IgG subclass responses as compared with PBS control (condition 1), which is consistent with the results in Fig. 2B. In summary, this study on IgG subclasses clearly revealed that the form of Ags could bias the distributions of IgG subclasses elicited upon immunization, and p-liposome$_{20\%\text{-m}}$ alone could trigger the production of IgG1 in the absence of T cell help.

Ag-specific B cells revealed by flow cytometry

To further examine the mechanisms involved in this production of class-switched Abs, we have developed a dual-functional liposome, named fp-liposome$_{6\%\text{-m}}$ in this article, for tracking of Ag-specific B cells using flow cytometry (*Materials and Methods*). This dual-functional liposome encapsulated the fluorescent dye Alexa Fluor 594 in the interior of the liposome, whose surface was also covalently conjugated with the aforementioned TNF-α peptide. Therefore, we expect that this dual-functional liposome can bind to TNF-α specific B cells and serve as a fluorescent indicator to reveal these Ag-specific B cells via flow cytometry. To this end, we inoculated C57BL/6 wild-type mice with PBS, p-liposome$_{20\%\text{-m}}$, or p-VLP$_{Q\beta}$, respectively. On day 4 after inoculation, we prepared single-cell suspensions of splenocytes, incubated them with fp-liposome$_{6\%\text{-m}}$, together with markers for mouse CD19, and subjected the cells to flow cytometry. As shown in Fig. 9, control mice inoculated with PBS showed negligible amounts of B cell populations that were specific for the fluorescent liposome (Q2 in Fig. 9A), whereas mice inoculated with either p-liposome$_{20\%\text{-m}}$ (Fig. 9B) or p-VLP$_{Q\beta}$ (Fig. 9C) showed reproducible B cell populations that were specific for fp-liposome$_{6\%\text{-m}}$. The percentages of these populations were significantly higher than those of control mice inoculated with PBS (Fig. 9D). This difference suggests that the TNF-α–specific B cells were triggered to expand after relevant Ag exposure, which allowed them to be detected above background. Furthermore, the fraction of TNF-α–specific B cells from mice inoculated with p-VLP$_{Q\beta}$ was ~3-fold of that from mice inoculated with p-liposome$_{20\%\text{-m}}$, which was qualitatively consistent with ELISA results. This study thus supports that Ag-specific B cells can expand upon exposure to the liposomal self-antigen in vivo, and these B cells can be detected as early as day 4 after immunization.

No germinal center formation above background upon p-liposome$_{20\%\text{-m}}$ immunization

Induction of germinal centers is a hallmark of humoral immune responses to foreign Ags. We asked whether germinal centers were formed in response to vaccination with self-antigen displaying liposomes. To address this question, we inoculated C57BL/6 wild-type mice with PBS control, p-liposome$_{20\%\text{-m}}$, or p-VLP$_{Q\beta}$, respectively. On day 12 after inoculation, we prepared single-cell suspensions of splenocytes, incubated them with markers for mouse CD19 and GL7 Ag, and subjected the cells to flow cytometry. As shown in Fig. 10, control mice inoculated with PBS did show a low percentage of GL7$^+$ B cells, which might correspond to background level activation of B cells (Fig. 10A). However, mice inoculated with p-liposome$_{20\%\text{-m}}$ also showed comparable level of GL7$^+$ B cells (Fig. 10B). This level of activation was statistically indistinguishable from that of PBS control (Fig. 10D), suggesting that inoculation of p-liposome$_{20\%\text{-m}}$ alone did not bring up the level of B cell activation above background on day 12 after inoculation. In contrast, GL7$^+$ B cell population was evident in mice immunized with p-VLP$_{Q\beta}$ (Fig. 10C), which was statistically higher than either PBS control or the mice immunized with p-liposome$_{20\%\text{-m}}$ (Fig. 10D). These results indicate that there was no formation of stable germinal centers that could be distinguished from background on day 12 after inoculation of the liposomal self-antigen. These results were also qualitatively consistent with the fact that no apparent increase of Ab titer was observed for

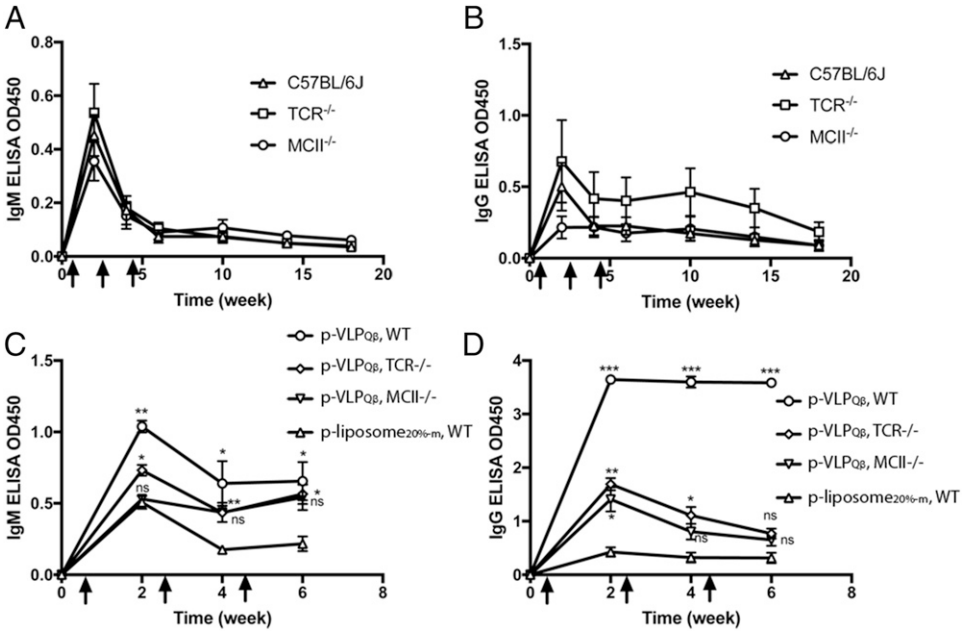

FIGURE 7. Comparison of anti–TNF-α peptide Ab response in gene knockout mice with wild-type C57BL/6. (**A** and **B**) Three groups of mice were inoculated with the same dose of p-liposome$_{20\%\text{-m}}$ (4.5 μg TNF-α peptide) following the same schedule: wild-type (C57BL/6J), TCR$^{-/-}$, and MCII$^{-/-}$ mice. The upward arrows denote the time of inoculations. Time courses of ELISA OD values for IgM (A) and IgG (B) measured from 1:100 diluted mouse sera, collected at weeks 2, 4, and 6, 11 d after each immunization, and weeks 10, 14, and 18 after the first inoculation. Each data point in the figures represents the mean of OD450 values obtained from four mice of each group ($n = 4$). Error bars represent the SEs. One-way ANOVA was conducted for sera from three mice groups collected at the same time point, and p values are >0.05 for all six groups at weeks 2, 4, 6, 10, 14, and 18. (**C** and **D**) Three groups of mice were inoculated with the same dose of p-VLP$_{Q\beta}$ (0.5 μg TNF-α peptide) following the same schedule: wild-type mice (C57BL/6J, circles), TCR$^{-/-}$ mice (diamond), and MCII$^{-/-}$ mice (down triangle). The upward arrows denote the time of inoculations. Time courses of ELISA OD values for IgM (C) and IgG (D) measured from 1:100 diluted mouse sera, collected at weeks 2, 4, and 6, 11 d after each immunization. Each data point in the figures represents the mean of OD450 values obtained from four mice of each group ($n = 4$). Error bars represent the SEs. Data from p-liposome$_{20\%\text{-m}}$ (4.5 μg TNF-α peptide) were also plotted in (C) and (D) for comparison purpose (upper triangle). For (C) and (D), p-liposome$_{20\%\text{-m}}$ was used as a reference to determine statistical difference between data points by Student t test. $^{***}p < 0.001$, $^{**}p < 0.01$, $^{*}p < 0.05$. ns, not significant ($p > 0.05$).

the IgG Abs elicited upon repeated inoculation of the liposomal Ag (Fig. 2).

Discussion

The response of B cells to particulate Ags is highly relevant to both our understanding of host immune responses toward viruses and rationale design of vaccines. In this study, we have used carefully engineered liposomal nanoparticles that display a model self-antigen peptide at tailored densities to investigate the factors that lead to Ab responses. In our particle design, we have chosen maleimide chemistry for conjugation of the self-antigen onto liposomal surface. This covalent conjugation ensures the density of Ag is stable with time (Fig. 1F), which is in contrast to the alternative noncovalent Ni-NTA technology, where the epitope density will decrease rapidly upon dilution into biological milieu (15). The stability of epitope density on these particles, therefore, allows us to interpret our results based on varied epitope densities with confidence.

When the epitope density exceeded certain threshold, these liposomal particles could elicit both IgM and IgG autoreactive Abs in the absence of any adjuvants. In particular, we identified a threshold condition in which IgG response was no longer significant despite the fact that these liposomal particles carried 360 ± 64 molecules of the antigenic peptides per particle on average (Fig. 3B). The IgG response was also elicited in two lines of gene knockout mice that were defective in either TCRs or MHC class II molecules on B cells, which further uncovered that this class switching is independent of cognate T cells. These conclusions were further supported by flow cytometry experiments in which we could detect TNF-α–specific B cells in mice as early as day 4 after immunization with the liposomal Ag (Fig. 9B). The absence of these B cells in control mice suggest that these cells arose as a result of expansion in response to the specific Ag exposure. Altogether, these results provided an experimental validation for the hypothesis that epitope density could serve as a stand-alone signal (1) to trigger B cell secretion of class-switched IgG against a self-antigen in vivo, independent of cognate T cell help and in the absence of any other adjuvants. The profiles of IgG subclasses induced by the liposomal self-antigen include IgG1, IgG2b, and Ig3 (Fig. 8), which are different from the classic type II T-independent Ags, such as NP-Ficoll, and suggest a different mechanism involved in this IgG elicitation.

Class-switch recombination (CSR) provides the immune system with Abs of different effector functions (41). IgG, in particular, offers benefits over IgM, because its smaller size can easily gain access to extravascular space and offers protection at those sites (42). In addition, class-switched B cells may also gain advantage in signaling and survival over unswitched B cells because of the difference in Ig cytoplasmic tail (43). Although CSR can be conveniently induced in cell culture using TLR ligands, the signal(s) to trigger CSR in vivo has been less clear (44). It was reported that gut B cells can undergo CSR to produce IgA in the absence of CD40 signaling or germinal center formation (45). Additionally, evidence suggesting that B-1 B cells and marginal zone B cells could produce class-switched IgG and IgA Abs through T cell–independent pathways has been reported (46), although the order of molecular events that led to these T cell–independent CSR was not clear. In a recent study, it was shown

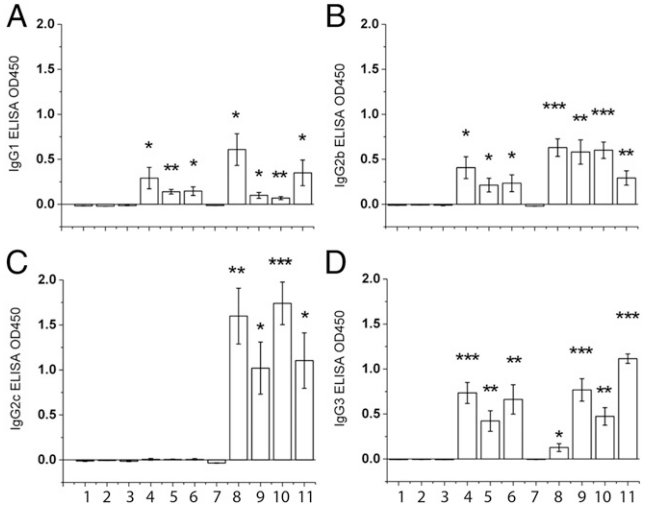

FIGURE 8. Anti–TNF-α peptide IgG subclasses in mice measured 11 d after first inoculation with various agents. (**A**–**D**) ELISA OD values for IgG1 (A), IgG2b (B), IgG2c (C), and IgG3 (D), respectively. The conditions 1–11 are PBS injection of C57BL/6 wild-type mice (1), liposome only injection of C57BL/6 wild-type mice (2), soluble peptides injection of C57BL/6 wild-type mice (3), p-liposome$_{20\%\text{-m}}$ injection of C57BL/6 wild-type mice (4), p-liposome$_{20\%\text{-m}}$ injection of TCR$^{-/-}$ mice (5), p-liposome$_{20\%\text{-m}}$ injection of MCII$^{-/-}$ mice (6), VLP$_{Q\beta}$ and soluble peptide injection of C57BL/6 wild-type mice (7), p-VLP$_{Q\beta}$ injection of C57BL/6 wild-type mice (8), p-VLP$_{Q\beta}$ injection of TCR$^{-/-}$ mice (9), p-VLP$_{Q\beta}$ injection of MCII$^{-/-}$ (10), and p-liposome$_{20\%\text{-m}}$ and CpG injection of C57BL/6 wild-type mice (11). Throughout, the Ab responses were from 1:100 diluted mouse sera, except condition 8, in which 1:1600 diluted sera were used to avoid the saturation of ELISA readings. The dose of TNF-α peptide per injection was 4.5 μg for conditions 3, 4, 5, 6, and 11, whereas the dose of TNF-α peptide per injection was 0.5 μg for conditions 7, 8, 9, and 10. For condition 11, 20 μg CpG was mixed with p-liposome$_{20\%\text{-m}}$ before inoculation. (A–D) Soluble peptides (condition 3) was used as a reference to determine statistical difference between data points by Student *t* test. Error bars represent the SEs ($n = 4$). The IgG1 response in gene knockout mice (conditions 5, 6, 9, and 10) were low in magnitudes. However, these responses were reproduced in an independent repeat of the experiments using a second set of animals and statistically significant compared with those from soluble peptides. $^{***}p < 0.001$, $^{**}p < 0.01$, $^{*}p < 0.05$.

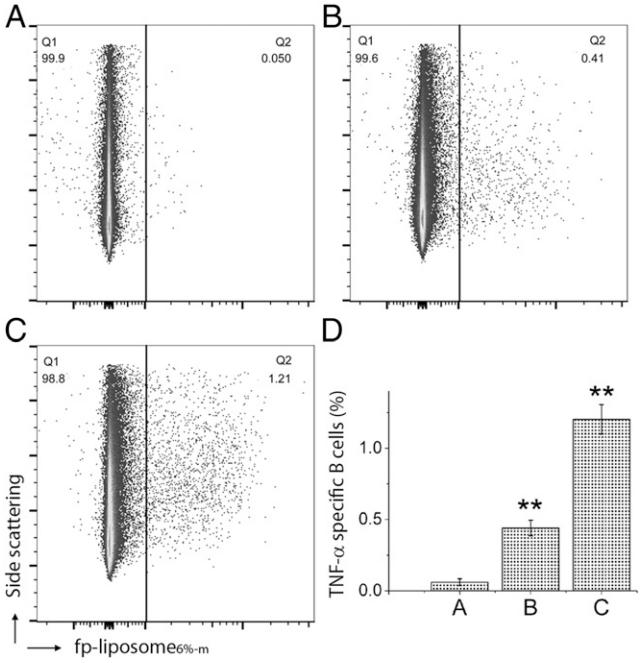

FIGURE 9. Flow cytometry analysis of TNF-α–specific B cells from splenocytes on day 4 after inoculation with various reagents. (**A**–**C**) CD19^{+} B cells from mouse splenocytes harvested on day 4 after inoculation with PBS (A) (100 μl), p-liposome$_{20\%\text{-m}}$ (B), or p-VLP$_{Q\beta}$ (C). The number of events shown in (A)–(C) are 101,997, 172,028, and 124,628, respectively. The dose of TNF-α peptide was 4.5 μg for (B) and 0.5 μg for (C), respectively. The cytograms were gated for TNF-α peptide–specific populations, indicated by Q2 in (A)–(C). The percentages of TNF-α–specific B cells from Q2 are further shown and compared in (**D**). PBS-inoculated mice were used as a reference to determine statistical difference between data points by Student *t* test in (D). Error bars represent the SEs ($n = 4$). $^{**}p < 0.01$.

that VLP$_{Q\beta}$ could induce class-switched and somatically mutated memory B cells in the absence of T cell help and also Bcl-6 expression in pregerminal center B cells (47). However, because Qβ viral-like particles possess both high epitope density and ssRNA packaged inside the particles, which could serve as a potent TLR 7 ligand, it remains unclear if epitope density alone could trigger CSR in the absence of T cells in vivo.

The results from current study show that epitope density is a distinct signal that can trigger B cell activation and secretion of class-switched IgG in vivo, independent of the cognate interactions with helper T cells and other adjuvants such as TLR ligands. Whether this phenomenon is extensible to other Ags in general remains to be determined in the future. However, if it were true for other Ags, it could provide benefits to the immune system for fending various viral agents that typically display a dense array of epitopes on particle surface (1). Different viral strains carry surface Ags of different structures. Although it may take time for affinity maturation to develop a perfect Ab against the different structures of viral surface Ags, to recognize and respond to the epitope density, a common feature of most viral agents, might offer a good strategy. Upon initial recognition of the epitopes on particulate Ags, although the affinity toward individual epitope is low, the epitope density can drive B cell response quickly in the absence of T cells to secrete both IgM and class-switched IgG Abs. The IgG response, even in the absence of affinity maturation, may play important roles in B cell functionality and also the control of pathogen proliferation during early phases of infection. For example, it was observed that influenza-specific IgG responses could be mounted in influenza-infected mice that were defective in cognate T cell help (48). Although this CD4 T cell–independent IgG Ab response was low in its titer, it could promote resolution of primary influenza virus infection and help prevent reinfection in mice (48). The signal(s) to trigger the production of the influenza-specific IgG in the absence of T cell help was unclear. However, based on current studies, it is tempting to speculate that this CD4 T cell–independent IgG Ab may arise from the mechanism that we hypothesized above (i.e., a threshold density of influenza-specific surface Ags such as the hemagglutinin or the neuraminidase, which is a subject for future research).

The results described in this work also open up several important questions that are worth studying in the future. First, are there particular subsets of B cells required for the T cell–independent IgG response observed in current study? Marginal zone B cells play critical roles in early response to T-independent particulate Ags (49, 50). The ability to track Ag-specific B cells using flow cytometry (Fig. 9) offers a potential way to identify those cells early on during this activation process and examine their status of B cell activation upon Ag exposure. Second, are other cells, such as dendritic cells, required for this T cell–independent IgG response? This question is relevant, because dendritic cells have been implicated in the T-independent class switching of B1 and

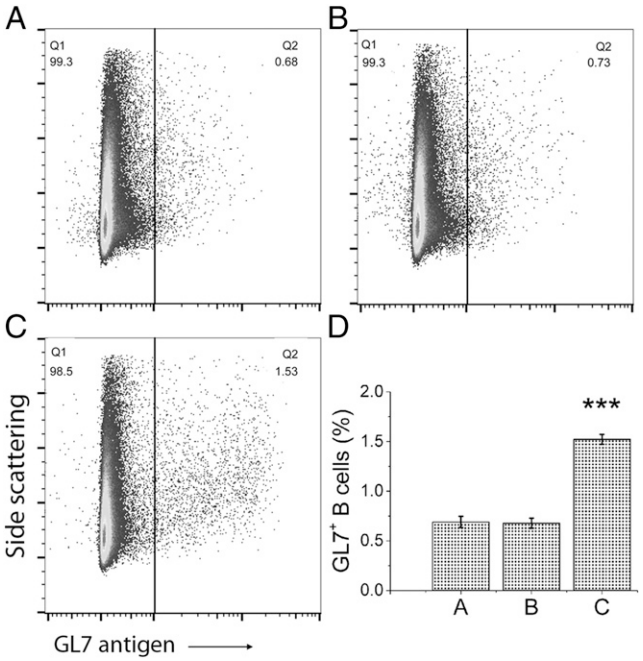

FIGURE 10. Flow cytometry analysis of GL7 Ag–positive B cells from splenocytes on day 12 after inoculation with various reagents. (**A**–**C**) $CD19^+$ B cells from mouse splenocytes harvested on day 12 after inoculation with PBS (A) (100 μl), p-liposome$_{20\%\text{-m}}$ (B), or p-$VLP_{Q\beta}$ (C). The number of events shown in (A)–(C) are 126,549, 128,190, and 114,264, respectively. The dose of TNF-α peptide was 4.5 μg for (B) and 0.5 μg for (C), respectively. The cytograms were further gated for $GL7^+$ populations, indicated by Q2 in (A)–(C). The percentages of $GL7^+$ B cells from Q2 are further shown and compared in (**D**). PBS-inoculated mice were used as a reference to determine statistical difference between data points by Student *t* test in (D). Error bars represent the SEs ($n = 4$). $^{***}p < 0.001$.

marginal zone B cells (44). In contrast, recent studies by Hong et al. (51) have clearly demonstrated that Ag-specific B cells themselves are essential and sufficient to present Ags to naive $CD4^+$ T cells and initiate antiviral response in lieu of dendritic cells that are thought by many as required for the initiation of $CD4^+$ T cell activation. These studies, thus, uncovered novel aspects of B cell function in humoral immunity, and in the future, it will be relevant to study the impact of epitope density on B cell secretion of cytokines, because differences in cytokine secretion by B cells may well signal other immune cells for collaborative efforts to contain the invading pathogens in a timely manner.

Our current study also suggests that high epitope density alone may break B cell tolerance in the absence of cognate T cell help or any other adjuvants in vivo. The model Ag that we employed in this study was a peptide derived from mouse TNF-α protein, a proinflammatory cytokine that is important in the pathogenesis of a number of chronic inflammatory diseases (52). Although the in vivo concentration of this protein that is required to develop B cell tolerance toward this protein has not been determined, our results indicate that potentially self-reactive B cells are available that can be activated by particulate Ags that display relevant self-epitopes above a threshold of epitope density in the absence of any other adjuvants. In fact, the ability of the IgG to bind to the rTNF-α protein in our studies further supports this hypothesis. The implication of this result on the maintenance of B cell tolerance also warrants future studies.

Compared with the IgG response elicited by viral-like particles in wild-type mice, the IgG titer from the above T-independent B cell activation is lower by two to three orders of magnitudes (Fig. 4E). Consistent with this phenomenon, we could not detect germinal center formation above background in mice on day 12 after inoculation of the liposomal self-antigen (Fig. 10). Strikingly, when the Ag-conjugated viral-like particles were administered into gene knockout mice that were deficient in T cell help, the IgG response fell to a level that could be compared with that of liposomal nanoparticles within the same order of magnitudes. The results clearly illustrate that T cell help dominates the IgG response to viral-like particles in wild-type mice, and the major difference between Ag-conjugated viral-like particles and liposomal particles is their differential ability to recruit T cell help and maintain germinal centers after the initial B cell activation.

It is worth noting, however, that our current results do not exclude the possibility of transient formation of germinal centers upon Ag exposure. Germinal center formation in response to T-independent Ags has been reported (53, 54). In particular, a study led by MacLennan (55) showed that large germinal centers could form in the absence of T cells in response to NP-Ficoll, although these germinal centers aborted abruptly on day 5 after immunization (55). The formation of these transient germinal centers required the multivalent nature of the Ag, a threshold of the Ag dose, and also a threshold frequency of Ag-specific B cells. The Ag dose that we have used in current studies is more than 6-fold lower than the Ag dose used in those studies. Studies are underway to examine if germinal center structures may have formed even transiently in response to the liposomal self-antigens and if there is any effect of Ag dose on this process.

The molecular components or features of viral-like particles that are critical for this T cell recruitment remains to be determined in the future. Among other things, two potential factors that may come into play are the following: 1) the rigidity of epitope display, and 2) the presence of nucleic acids in viral-like particles that may synergize B cell activation through the engagement of TLR. In particular, substantial studies have supported the role of TLR 9 ligands in augmenting B cell antiviral responses (56).

In summary, we showed that a peptide derived from a self-antigen, upon conjugation to liposomes above a threshold of epitope density, could induce class-switched Ab responses in the absence of cognate T cell help or other adjuvants. To the best of our knowledge, this is the first time that the epitope density was shown to be a stand-alone signal to trigger B cell secretion of class-switched Abs in vivo in the absence of T cells. Our study has thus uncovered a fundamental aspect regarding B cell activation in vivo and offered valuable insights to future vaccine design targeting self-antigens, which could be useful in treating diseases in which self-antigens are associated, such as rheumatoid arthritis and Alzheimer disease.

Acknowledgments

We thank Amanda Ames for help on ELISA, James Wang for help in preparation of TNF-α peptide–conjugated liposomes, and Cheng Laboratory members for helpful discussions.

Disclosures

The authors have no financial conflicts of interest.

References

1. Cheng, W. 2016. The density code for the development of a vaccine? *J. Pharm. Sci.* 105: 3223–3232.
2. Bachmann, M. F., U. H. Rohrer, T. M. Kündig, K. Bürki, H. Hengartner, and R. M. Zinkernagel. 1993. The influence of antigen organization on B cell responsiveness. *Science* 262: 1448–1451.
3. Chackerian, B., P. Lenz, D. R. Lowy, and J. T. Schiller. 2002. Determinants of autoantibody induction by conjugated papillomavirus virus-like particles. *J. Immunol.* 169: 6120–6126.

4. Chackerian, B., D. R. Lowy, and J. T. Schiller. 1999. Induction of autoantibodies to mouse CCR5 with recombinant papillomavirus particles. *Proc. Natl. Acad. Sci. USA* 96: 2373–2378.
5. Chackerian, B., D. R. Lowy, and J. T. Schiller. 2001. Conjugation of a self-antigen to papillomavirus-like particles allows for efficient induction of protective autoantibodies. *J. Clin. Invest.* 108: 415–423.
6. Lechner, F., A. Jegerlehner, A. C. Tissot, P. Maurer, P. Sebbel, W. A. Renner, G. T. Jennings, and M. F. Bachmann. 2002. Virus-like particles as a modular system for novel vaccines. *Intervirology* 45: 212–217.
7. Chackerian, B. 2007. Virus-like particles: flexible platforms for vaccine development. *Expert Rev. Vaccines* 6: 381–390.
8. Cartwright, B., C. J. Smale, F. Brown, and R. Hull. 1972. Model for vesicular stomatitis virus. *J. Virol.* 10: 256–260.
9. Baker, T. S., W. W. Newcomb, N. H. Olson, L. M. Cowsert, C. Olson, and J. C. Brown. 1991. Structures of bovine and human papillomaviruses. Analysis by cryoelectron microscopy and three-dimensional image reconstruction. *Biophys. J.* 60: 1445–1456.
10. Jegerlehner, A., T. Storni, G. Lipowsky, M. Schmid, P. Pumpens, and M. F. Bachmann. 2002. Regulation of IgG antibody responses by epitope density and CD21-mediated costimulation. *Eur. J. Immunol.* 32: 3305–3314.
11. Desaymard, C., and M. Feldmann. 1975. Role of epitope density in the induction of immunity and tolerance with thymus-independent antigens. I. Studies with 2,4-dinitrophenyl conjugates in vitro. *Eur. J. Immunol.* 5: 537–541.
12. Desaymard, C., and J. G. Howard. 1975. Role of epitope density in the induction of immunity and tolerance with thymus-independent antigens. II. Studies with 2,4-dinitrophenyl conjugates in vivo. *Eur. J. Immunol.* 5: 541–545.
13. Turner, J. S., M. Marthi, Z. L. Benet, and I. Grigorova. 2017. Transiently antigen-primed B cells return to naive-like state in absence of T-cell help. *Nat. Commun.* 8: 15072.
14. Watson, D. S., A. N. Endsley, and L. Huang. 2012. Design considerations for liposomal vaccines: influence of formulation parameters on antibody and cell-mediated immune responses to liposome associated antigens. *Vaccine* 30: 2256–2272.
15. Chen, Z., J. J. Moon, and W. Cheng. 2018. Quantitation and stability of protein conjugation on liposomes for controlled density of surface epitopes. *Bioconjug. Chem.* 29: 1251–1260.
16. Phelps, E. A., N. O. Enemchukwu, V. F. Fiore, J. C. Sy, N. Murthy, T. A. Sulchek, T. H. Barker, and A. J. Garcia. 2012. Maleimide cross-linked bioactive PEG hydrogel exhibits improved reaction kinetics and cross-linking for cell encapsulation and in situ delivery. *Adv. Mater.* 24: 64–70
17. Stewart, J. C. 1980. Colorimetric determination of phospholipids with ammonium ferrothiocyanate. *Anal. Biochem.* 104: 10–14.
18. Smith, P. K., R. I. Krohn, G. T. Hermanson, A. K. Mallia, F. H. Gartner, M. D. Provenzano, E. K. Fujimoto, N. M. Goeke, B. J. Olson, and D. C. Klenk. 1985. Measurement of protein using bicinchoninic acid. *Anal. Biochem.* 150: 76–85.
19. Morton, R. E., and T. A. Evans. 1992. Modification of the bicinchoninic acid protein assay to eliminate lipid interference in determining lipoprotein protein content. *Anal. Biochem.* 204: 332–334.
20. Schägger, H. 2006. Tricine-SDS-PAGE. *Nat. Protoc.* 1: 16–22.
21. Van Rompay, K. K., Z. Hunter, K. Jayashankar, J. Peabody, D. Montefiori, C. C. LaBranche, B. F. Keele, K. Jensen, K. Abel, and B. Chackerian. 2014. A vaccine against CCR5 protects a subset of macaques upon intravaginal challenge with simian immunodeficiency virus SIVmac251. *J. Virol.* 88: 2011–2024.
22. Mombaerts, P., A. R. Clarke, M. A. Rudnicki, J. Iacomini, S. Itohara, J. J. Lafaille, L. Wang, Y. Ichikawa, R. Jaenisch, M. L. Hooper, et al. 1992. Mutations in T-cell antigen receptor genes alpha and beta block thymocyte development at different stages. [Published erratum appears in 1992 *Nature* 360: 491.] *Nature* 360: 225–231.
23. Fikrig, E., S. W. Barthold, M. Chen, C. H. Chang, and R. A. Flavell. 1997. Protective antibodies develop, and murine Lyme arthritis regresses, in the absence of MHC class II and CD4+ T cells. *J. Immunol.* 159: 5682–5686.
24. Frey, A., J. Di Canzio, and D. Zurakowski. 1998. A statistically defined endpoint titer determination method for immunoassays. *J. Immunol. Methods* 221: 35–41.
25. Hedman, K., and I. Seppälä. 1988. Recent rubella virus infection indicated by a low avidity of specific IgG. *J. Clin. Immunol.* 8: 214–221.
26. Taylor, K. M. G., and R. M. Morris. 1995. Thermal-analysis of phase-transition behavior in liposomes. *Thermochim. Acta* 248: 289–301.
27. Banner, D. W., A. D'Arcy, W. Janes, R. Gentz, H. J. Schoenfeld, C. Broger, H. Loetscher, and W. Lesslauer. 1993. Crystal structure of the soluble human 55 kd TNF receptor-human TNF beta complex: implications for TNF receptor activation. *Cell* 73: 431–445.
28. Hu, S., S. Liang, H. Guo, D. Zhang, H. Li, X. Wang, W. Yang, W. Qian, S. Hou, H. Wang, et al. 2013. Comparison of the inhibition mechanisms of adalimumab and infliximab in treating tumor necrosis factor α-associated diseases from a molecular view. *J. Biol. Chem.* 288: 27059–27067.
29. Spohn, G., R. Guler, P. Johansen, I. Keller, M. Jacobs, M. Beck, F. Rohner, M. Bauer, K. Dietmeier, T. M. Kündig, et al. 2007. A virus-like particle-based vaccine selectively targeting soluble TNF-alpha protects from arthritis without inducing reactivation of latent tuberculosis. *J. Immunol.* 178: 7450–7457.
30. Klibanov, A. L., K. Maruyama, V. P. Torchilin, and L. Huang. 1990. Amphipathic polyethyleneglycols effectively prolong the circulation time of liposomes. *FEBS Lett.* 268: 235–237.
31. Blume, G., and G. Cevc. 1990. Liposomes for the sustained drug release in vivo. *Biochim. Biophys. Acta* 1029: 91–97.
32. Allen, T. M., C. Hansen, F. Martin, C. Redemann, and A. Yau-Young. 1991. Liposomes containing synthetic lipid derivatives of poly(ethylene glycol) show prolonged circulation half-lives in vivo. *Biochim. Biophys. Acta* 1066: 29–36.
33. Maruyama, K., T. Yuda, A. Okamoto, C. Ishikura, S. Kojima, and M. Iwatsuru. 1991. Effect of molecular weight in amphipathic polyethyleneglycol on prolonging the circulation time of large unilamellar liposomes. *Chem. Pharm. Bull. (Tokyo)* 39: 1620–1622.
34. Senior, J., C. Delgado, D. Fisher, C. Tilcock, and G. Gregoriadis. 1991. Influence of surface hydrophilicity of liposomes on their interaction with plasma protein and clearance from the circulation: studies with poly(ethylene glycol)-coated vesicles. *Biochim. Biophys. Acta* 1062: 77–82.
35. Eisen, H. N., and G. W. Siskind. 1964. Variations in affinities of antibodies during the immune response. *Biochemistry* 3: 996–1008.
36. Tissot, A. C., P. Maurer, J. Nussberger, R. Sabat, T. Pfister, S. Ignatenko, H. D. Volk, H. Stocker, P. Müller, G. T. Jennings, et al. 2008. Effect of immunisation against angiotensin II with CYT006-AngQb on ambulatory blood pressure: a double-blind, randomised, placebo-controlled phase IIa study. *Lancet* 371: 821–827.
37. Hunter, Z., E. Tumban, A. Dziduszko, and B. Chackerian. 2011. Aerosol delivery of virus-like particles to the genital tract induces local and systemic antibody responses. *Vaccine* 29: 4584–4592.
38. Sakaguchi, S., T. Yamaguchi, T. Nomura, and M. Ono. 2008. Regulatory T cells and immune tolerance. *Cell* 133: 775–787.
39. Vita, R., S. Mahajan, J. A. Overton, S. K. Dhanda, S. Martini, J. R. Cantrell, D. K. Wheeler, A. Sette, and B. Peters. 2019. The immune epitope database (IEDB): 2018 update. *Nucleic Acids Res.* 47: D339–D343.
40. Tesch, H., F. I. Smith, W. J. Müller-Hermes, and K. Rajewsky. 1984. Heterogeneous and monoclonal helper T cells induce similar anti-(4-hydroxy-3-nitrophenyl)acetyl (NP) antibody populations in the primary adoptive response. I. Isotype distribution. *Eur. J. Immunol.* 14: 188–194.
41. Stavnezer, J., and C. E. Schrader. 2014. IgH chain class switch recombination: mechanism and regulation. *J. Immunol.* 193: 5370–5378.
42. Xu, Z., H. Zan, E. J. Pone, T. Mai, and P. Casali. 2012. Immunoglobulin class-switch DNA recombination: induction, targeting and beyond. *Nat. Rev. Immunol.* 12: 517–531.
43. Kaisho, T., F. Schwenk, and K. Rajewsky. 1997. The roles of gamma 1 heavy chain membrane expression and cytoplasmic tail in IgG1 responses. *Science* 276: 412–415.
44. Cerutti, A., I. Puga, and M. Cols. 2011. Innate control of B cell responses. *Trends Immunol.* 32: 202–211.
45. Bergqvist, P., E. Gärdby, A. Stensson, M. Bemark, and N. Y. Lycke. 2006. Gut IgA class switch recombination in the absence of CD40 does not occur in the lamina propria and is independent of germinal centers. *J. Immunol.* 177: 7772–7783.
46. Fagarasan, S., and T. Honjo. 2000. T-Independent immune response: new aspects of B cell biology. *Science* 290: 89–92.
47. Liao, W., Z. Hua, C. Liu, L. Lin, R. Chen, and B. Hou. 2017. Characterization of T-dependent and T-independent B cell responses to a virus-like particle. *J. Immunol.* 198: 3846–3856.
48. Lee, B. O., J. Rangel-Moreno, J. E. Moyron-Quiroz, L. Hartson, M. Makris, F. Sprague, F. E. Lund, and T. D. Randall. 2005. CD4 T cell-independent antibody response promotes resolution of primary influenza infection and helps to prevent reinfection. *J. Immunol.* 175: 5827–5838.
49. Martin, F., and J. F. Kearney. 2002. Marginal-zone B cells. *Nat. Rev. Immunol.* 2: 323–335.
50. Martin, F., A. M. Oliver, and J. F. Kearney. 2001. Marginal zone and B1 B cells unite in the early response against T-independent blood-borne particulate antigens. *Immunity* 14: 617–629.
51. Hong, S., Z. Zhang, H. Liu, M. Tian, X. Zhu, Z. Zhang, W. Wang, X. Zhou, F. Zhang, Q. Ge, et al. 2018. B cells are the dominant antigen-presenting cells that activate naive $CD4^+$ T cells upon immunization with a virus-derived nanoparticle antigen. *Immunity* 49: 695–708.e4.
52. Klareskog, L., and H. McDevitt. 1999. Rheumatoid arthritis and its animal models: the role of TNF-alpha and the possible absence of specific immune reactions. *Curr. Opin. Immunol.* 11: 657–662.
53. Wang, D., S. M. Wells, A. M. Stall, and E. A. Kabat. 1994. Reaction of germinal centers in the T-cell-independent response to the bacterial polysaccharide alpha(1-->6)dextran. *Proc. Natl. Acad. Sci. USA* 91: 2502–2506.
54. Sverremark, E., and C. Fernandez. 1998. Role of T cells and germinal center formation in the generation of immune responses to the thymus-independent carbohydrate dextran B512. *J. Immunol.* 161: 4646–4651.
55. de Vinuesa, C. G., M. C. Cook, J. Ball, M. Drew, Y. Sunners, M. Cascalho, M. Wabl, G. G. Klaus, and I. C. MacLennan. 2000. Germinal centers without T cells. *J. Exp. Med.* 191: 485–494.
56. Hou, B., P. Saudan, G. Ott, M. L. Wheeler, M. Ji, L. Kuzmich, L. M. Lee, R. L. Coffman, M. F. Bachmann, and A. L. DeFranco. 2011. Selective utilization of Toll-like receptor and MyD88 signaling in B cells for enhancement of the antiviral germinal center response. *Immunity* 34: 375–384.